Original Article

2-(8-Hydroxy-6-Methoxy-1-Oxo-1H-2-Benzopyran-3-yl) Propionic Acid, an Inhibitor of Angiogenesis, Ameliorates Renal Alterations in Obese Type 2 Diabetic Mice

Kunihiro Ichinose,[1] Yohei Maeshima,[1] Yoshihiko Yamamoto,[1] Masaru Kinomura,[1] Kumiko Hirokoshi,[1] Hiroyuki Kitayama,[1] Yuki Takazawa,[1] Hitoshi Sugiyama,[1] Yasushi Yamasaki,[1] Naoki Agata,[2] and Hirofumi Makino[1]

One of the mechanisms involved in the progression of diabetic nephropathy, the most common cause of end-stage renal failure, is angiogenic phenomenon associated with the increase of angiogenic factors such as vascular endothelial growth factor (VEGF)-A and angiopoietin (Ang)-2, an antagonist of Ang-1. In the present study, we examined the therapeutic efficacy of 2-(8-hydroxy-6-methoxy-1-oxo-1H-2-benzopyran-3-yl) propionic acid (NM-3), a small molecule isocoumarin with antiangiogenic activity, using diabetic *db/db* mice, a model of obese type 2 diabetes. Increases in kidney weight, glomerular volume, creatinine clearance, urinary albumin excretion, total mesangial fraction, glomerular type IV collagen, glomerular endothelial area ($CD31^+$), and monocyte/macrophage accumulation ($F4/80^+$) observed in control *db/db* mice were significantly suppressed by daily intraperitoneal injection of NM-3 (100 mg/kg, for 8 weeks). Increases in renal expression of VEGF-A, Ang-2, fibrogenic factor transforming growth factor (TGF)-β1, and chemokine monocyte chemoattractant protein-1 but not tumor necrosis factor-α were also inhibited by NM-3 in *db/db* mice. Furthermore, decreases of nephrin mRNA and protein levels in *db/db* mice were recovered by NM-3. In addition, treatment of *db/db* mice with NM-3 did not affect body weight, blood glucose, serum insulin, or food consumption. NM-3 significantly suppressed the increase of VEGF induced by high glucose in cultured podocytes and also suppressed the increase of VEGF and TGF-β induced by high glucose in cultured mesangial cells. Taken together, these results demonstrate the potential use of NM-3 as a novel therapeutic agent for renal alterations in type 2 diabetes. *Diabetes* 55: 1232–1242, 2006

Diabetic nephropathy is complicated in 30–40% of patients with type 2 diabetes and is the most common pathological disorder predisposing end-stage renal disease (ESRD) in Japan and the Western world. Early alterations in diabetic nephropathy include glomerular hyperfiltration, glomerular and tubular epithelial hypertrophy, glomerular basement membrane (GBM) thickening, and the development of microalbuminuria, followed by the development of the accumulation of mesangial matrix and overt proteinuria, eventually leading to glomerulosclerosis and ESRD (1). The involvement of various growth factors and cytokines, including angiotensin II, IGF-I, monocyte chemoattractant protein-1 (MCP-1), interleukin-6 (IL-6), and transforming growth factor (TGF)-β1, in the development of diabetic nephropathy have been reported (2).

Although angiogenesis, the development of new blood vessels from preexisting ones, plays a crucial role in physiological events, such as wound repair, uncontrolled neovascularization is associated with a number of pathological disorders, including tumor growth, rheumatoid arthritis, and diabetic retinopathy (3). Vascular endothelial growth factor (VEGF)-A, a potent stimulator of angiogenesis, promotes endothelial cell proliferation, migration, and endothelial cell tube formation (4). VEGF-A also induces vascular permeability (5) in association with inflammatory lesions. The protein and mRNA level of VEGF-A and its receptor flk-1/KDR were upregulated in experimental diabetic nephropathy (6–8). Studies using neutralizing anti–VEGF-A antibody further demonstrated the involvement of VEGF-A in early glomerular hypertrophy in type 1 diabetic model and mesangial matrix accumulation in the progressive stage of type 2 diabetic model (9,10).

Angiopoietin (Ang)-1, a major physiological ligand for endothelial receptor Tie2, induces the recruitment and stable attachment of pericytes leading to the maturation of newly formed blood vessels (11). In contrast, Ang-2 competitively inhibits the binding of Ang-1 to Tie2 and renders blood vessels "unstable" (12). Ang-2 loosens the attachment of pericytes and synergizes with VEGF-A to promote angiogenesis (12,13). However, when insufficient angiogenic stimuli are present, Ang-2 causes endothelial cell

From the [1]Department of Medicine and Clinical Science, Okayama University Graduate School of Medicine, Dentistry and Pharmaceutical Sciences, Okayama, Japan; and [2]Genzyme, Framingham, Massachusetts.

Address correspondence and reprint requests to Dr. Yohei Maeshima, Assistant Professor of Medicine, Department of Medicine and Clinical Science, Okayama University Graduate School of Medicine, Dentistry and Pharmaceutical Sciences, 2-5-1 Shikata-cho, Okayama, 700-8558, Japan. E-mail: ymaeshim@md.okayama-u.ac.jp.

Received for publication 19 October 2005 and accepted in revised form 30 January 2006.

K.I., Y.M., and Y.Yamam. contributed equally to this work.

Additional information for this article can be found in an online appendix at http://diabetes.diabetesjournals.org.

Ang, angiopoietin; CCr, creatinine clearance; ESRD, end-stage renal disease; GBM, glomerular basement membrane; IL-6, interleukin-6; MCP-1, monocyte chemoattractant protein-1; NM-3, 2-(8-hydroxy-6-methoxy-1-oxo-1H-2-benzopyran-3-yl) propionic acid; TGF, transforming growth factor; TNF-α, tumor necrosis factor-α; UACR, urinary albumin-to-creatinine ratio; VEGF, vascular endothelial growth factor.

DOI: 10.2337/db05-1367

TABLE 1
Body weight, blood glucose concentration, and food consumption

Group	Week 0			Week 8		
	Body weight (g)	Blood glucose (mmol/l)	Food consumption (g/24 h)	Body weight (g)	Blood glucose (mmol/l)	Food consumption (g/24 h)
Nondiabetic	21.3 ± 0.7	5.4 ± 0.5	5.1 ± 0.5	25.4 ± 1.0	5.4 ± 0.4	5.1 ± 0.4
Diabetic: placebo	39.3 ± 0.7*	20.8 ± 0.5*	7.5 ± 0.7*	48.4 ± 1.2*	20.5 ± 1.0*	8.0 ± 0.9*
Diabetic: NM-3	40.2 ± 0.6*	20.8 ± 1.3*	7.4 ± 1.0*	48.2 ± 1.4*	20.8 ± 0.7*	8.1 ± 0.7*

Data are means ± SE ($n = 6$ in each group). *$P < 0.01$ vs. nondiabetic controls.

apoptosis and vessel regression (12). During kidney development, Ang-1, Ang-2, and Tie2 are highly expressed and play pivotal roles in the maturation of glomeruli and renal blood vessels (14). We previously reported the upregulation of Ang-2 in the type 1 mouse diabetic nephropathy model, although the expression of Ang-1 was not altered (15,16).

Nephrin, a glomerular podocyte protein, is crucial for maintaining the integrity of the interpodocyte slit membrane structure and an intact filtration barrier. In diabetic nephropathy, the protein level of nephrin decreases possibly via the loss of nephrin into urine due to synthesis of the splice variant isoform of the nephrin lacking a transmembrane domain (17,18).

A previous study demonstrated that the increased glomerular filtration surface in diabetic nephropathy resulted from the formation of new glomerular capillaries in accordance with a slight elongation of the preexisting capillaries (19), analogous to the changes observed in pathological diabetic retinopathy.

2-(8-Hydroxy-6-methoxy-1-oxo-1H-2-benzopyran-3-yl) propionic acid (NM-3) is a novel synthetic derivative of cytogenin, a natural compound isolated from culture filtrate of *Streptoverticillium eurocidicum* (20,21). NM-3 potently inhibits endothelial cell proliferation, migration, sprouting, tube formation in vitro, and tumor growth in vivo (22). Moreover, NM-3 suppresses endothelial cell migration induced by VEGF and exerts inhibitory effects on angiogenesis in VEGF-secreting malignant tumors (21,22). A phase I clinical study of NM-3 in patients with cancer has demonstrated that NM-3 is a highly orally bioavailable and well-tolerated drug in humans (23). NM-3 is currently entering a phase II clinical trial in patients with multiple myeloma (24).

In the present study, to examine whether NM-3 could provide beneficial effects on type 2 diabetic nephropathy, we applied NM-3 to type 2 diabetic *db/db* mice. Here, we demonstrate that treatment with NM-3 markedly suppresses glomerular hypertrophy, hyperfiltration, and urinary albumin excretion as well as the expansion of mesangial matrix and the accumulation of monocytes/macrophages. These therapeutic effects are possibly mediated through the downregulation of proangiogenic signals induced by VEGF-A and Ang-2 and through the suppression of TGF-β1 and the recovery of nephrin.

RESEARCH DESIGN AND METHODS

The experimental protocol was approved by the Animal Ethics Review Committee of Okayama University. Adult female *db/db* mice (C57BL/KsJ-*db/db* Jcl; Clea Japan, Osaka, Japan) and their age-matched nondiabetic *db/m* littermates (C57BL/KsJ-*db/+m* Jcl; Clea Japan) were used in the present study. Mice were fed a standard pellet laboratory chow and were provided with water ad libitum. The *db/db* mice were included in this study at the age of 8 weeks because they develop diabetes (hyperglycemia) at the age of week 7–8 (25). At the age of 8 weeks, blood glucose of *db/db* mice was in the range of 20.3–22.1 mmol/l. Mice were divided into three subgroups ($n = 6$ for each subgroup): *1*) *db/db* mice treated with daily intraperitoneal injection of NM-3 (Genzyme, Cambridge, MA) at 100 mg · kg body wt^{-1} · day^{-1} for 8 weeks, *2*) *db/db* mice treated with daily intraperitoneal injection of vehicle buffer (PBS) for the same interval, and *3*) nondiabetic, control *db/m* mice receiving vehicle buffer.

Blood glucose was monitored every week. No mice died, and no signs of apparent exhaustion were observed during the experimental period. At 0 and 8 weeks after initiating the intraperitoneal injection of NM-3, the body weight and the individual 24-h food consumption were measured. At 8 weeks after initiating treatment, individual 24-h urine sample collection was performed using metabolic cages. Nonfasting blood samples were drawn from the retro-orbital venous plexus using heparinized capillary tubes under anesthesia at the time of death. Kidney, liver, and heart weights were measured just after death. NM-3 was dissolved in PBS and filtered to be used for the animal experiments. The dosage of NM-3 used in the present study was determined according to previous reports using NM-3 (22,26). NM-3 has a serum half-life of 3–10 h in preclinical models, a low toxicity profile, and thus a potentially wide therapeutic window (22). According to the manufacturer's information, oral dosage of NM-3 at 1 g/kg was well tolerated in animals without acute toxicity.

Blood and urine examination. Blood glucose was measured in tail-vein blood, and urine was tested for ketone bodies and glucose by SRL (Okayama, Japan). Serum and urinary creatinine levels were measured by the enzymatic colorimetric method as described previously (15). Urinary albumin concentration was measured by nephelometry (Organon Teknika-Cappel, Durham, NC) using anti-mouse albumin antibody (ICN Pharmaceuticals, Aurora, OH) as previously described (15). Results were normalized to the urinary creatinine levels and expressed as urinary albumin-to-creatinine ratio (UACR). The creatinine clearance (CCr) was calculated and expressed as milliliters per minute. Serum levels of mouse insulin were determined by enzyme-linked immunosorbent assay using an ultrasensitive rat insulin enzyme-linked immunosorbent assay kit and mouse insulin standard (Morinaga, Yokohama, Japan) following the manufacturer's instructions. According to the manufacturer's technical information, mouse insulin can be measured in combination with

TABLE 2
Mean serum insulin, liver weight, heart weight, and right kidney weight in experimental animals in week 8

Group	Serum insulin (mg/l)	Liver weight (mg)	Heart weight (mg)	Kidney weight (mg)
Nondiabetic	1.0 ± 0.2	1,133.6 ± 35.8	116.8 ± 1.3	155.6 ± 10.9
Diabetic: placebo	9.0 ± 1.3*	2,769.4 ± 285.8*	128.9 ± 13.5	230.7 ± 18.6*
Diabetic: NM-3	8.7 ± 0.4*	2,343.8 ± 89.3*	127.0 ± 5.3	211.8 ± 12.1*

Data are means ± SE ($n = 6$ in each group). *$P < 0.01$ vs. nondiabetic controls.

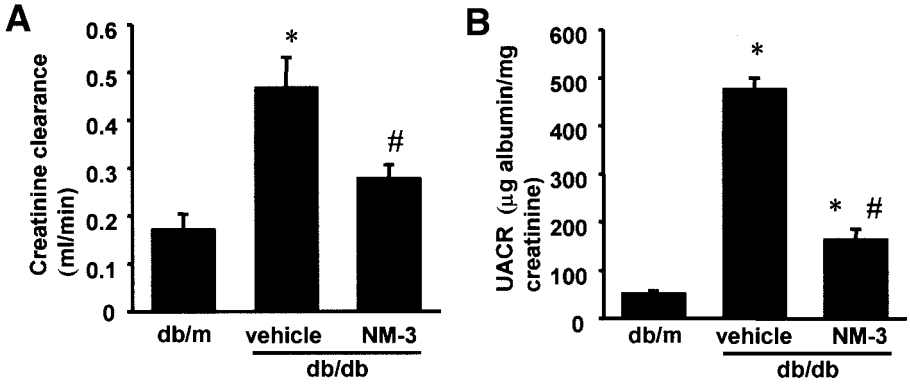

FIG. 1. ***A*****: Increase of CCr in** ***db/db*** **mice was partially suppressed by NM-3 (16 weeks of age). *P < 0.01 vs.** ***db/m*****; #P < 0.02 vs. vehicle.** ***B*****: Increase of UACR in** ***db/db*** **mice was significantly suppressed by treatment with NM-3. *P < 0.01 vs.** ***db/m*****; #P < 0.01 vs. vehicle. Vehicle,** ***db/db*** **mice treated with vehicle buffer; NM-3,** ***db/db*** **mice treated with NM-3.** ***n*** **= 6 for each group. Each column consists of means ± SE.**

mouse insulin standard because of a high homology among mammalian animals. All samples were examined in duplicate, and mean values of individual sera were used for statistical analysis. The intra- and interassay coefficients of variation for the insulin assays were <5 and 10%, respectively.

Histological analysis. At 8 weeks after starting treatment, kidneys were removed, fixed in 10% buffered formalin, and embedded in paraffin. Sections (4-μm) were stained with periodic acid Schiff for light microscopic observation to determine glomerular volume and mesangial matrix index as described previously (15,16) (online appendix [available at http://diabetes.diabetesjournals.org]).

Immunohistochemistry. Immunohistochemistry of CD31, type IV collagen, F4/80, and VEGF was performed using frozen sections as previously described (15,16,27,28) (online appendix).

RNA extraction and quantitative real-time PCR. RNA extraction and real-time PCR were performed to determine the mRNA levels of TGF-β1, IL-6, MCP-1, and nephrin in renal cortex as previously described (15,16) (online appendix).

Immunoblot. Immunoblot assay was performed to determine the protein levels of VEGF-A, Ang-1, Ang-2, nephrin, TGF-β, MCP-1, and tumor necrosis factor-α (TNF-α) in renal cortex as previously described (15,16,29–31) (online appendix).

Cell culture. Conditionally immortalized mouse podocytes (provided by Dr. Peter Mundel, Mount Sinai School of Medicine, New York, NY) and primary murine mesangial cells (MES13) were used to determine the direct effect of NM-3 on high glucose–induced increase of the protein levels of VEGF and/or TGF-β as previously described (32,33) (online appendix).

Statistical analysis. All values are expressed as means ± SE. A Kruskal-Wallis test with post hoc comparisons using the Scheffe's test was used for intergroup comparisons of multiple variables. Statistical analysis was performed by StatView software (Abacus Concepts, Berkeley, CA). A level of $P < 0.05$ was considered statistically significant.

RESULTS

Changes in blood glucose, body weight, food consumption, mean serum insulin, liver weight, heart weight, and kidney weight. Body weight, blood glucose, food consumption, serum levels of insulin, liver weight, heart weight, and kidney weight were significantly increased in *db/db* mice compared with *db/m* mice at the age of 16 weeks. Administration of NM-3 did not alter plasma glucose concentrations, food consumption, and mean serum insulin in *db/db* mice after 8 weeks of treatment (Tables 1 and 2). There was no significant difference in liver weight, heart weight, and kidney weight between treatments with NM-3 and vehicle. Kidney weight and liver weight tended to be lower in the NM-3–treated group compared with the vehicle-treated group (Table 2). Mean systolic blood pressure measured at the age of 16 weeks by a tail cuff method did not significantly differ among the experimental groups (*db/m* mice, 118 ± 5 mmHg; *db/db* mice treated with vehicle, 114 ± 3 mmHg; and *db/db* mice treated with NM-3, 112 ± 5 mmHg).

Changes in CCr and urinary albumin excretion. Serum creatinine levels did not significantly differ among the experimental groups. To evaluate the effect of NM-3 on preventing hyperfiltration associated with diabetic nephropathy, CCr and UACR were determined (Fig. 1). Although *db/db* mice treated with vehicle showed a marked elevation of CCr and UACR, NM-3 treatment

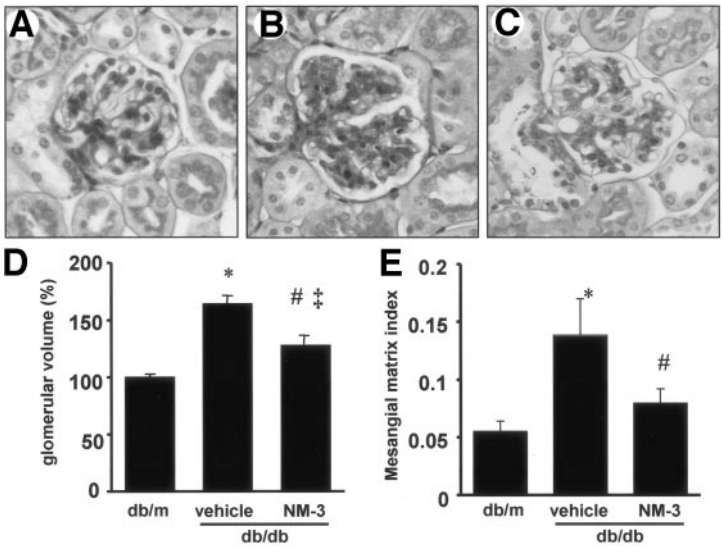

FIG. 2. ***A–C*****: Representative light microscopic appearance of glomeruli (periodic acid Schiff staining; original magnification ×400) for** ***db/m*** **mice (*A*),** ***db/db*** **mice treated with vehicle buffer (*B*), and** ***db/db*** **mice treated with NM-3 (*C*) at 16 weeks of age.** ***D*****: Increase of glomerular volume in** ***db/db*** **mice was diminished by treatment with NM-3. Glomerular volume was determined as described in RESEARCH DESIGN AND METHODS. *P < 0.05 vs.** ***db/m*****; #P < 0.05 vs. vehicle.** ***E*****: Mesangial matrix index was defined as the proportion of the glomerular tuft occupied by the mesangial matrix area (excluding nuclei). *P < 0.05 vs.** ***db/m*****; #P < 0.05 vs. vehicle.** ***n*** **= 6 for each group. Vehicle,** ***db/db*** **mice treated with vehicle buffer; NM-3,** ***db/db*** **mice treated with NM-3. Each column consists of means ± SE.**

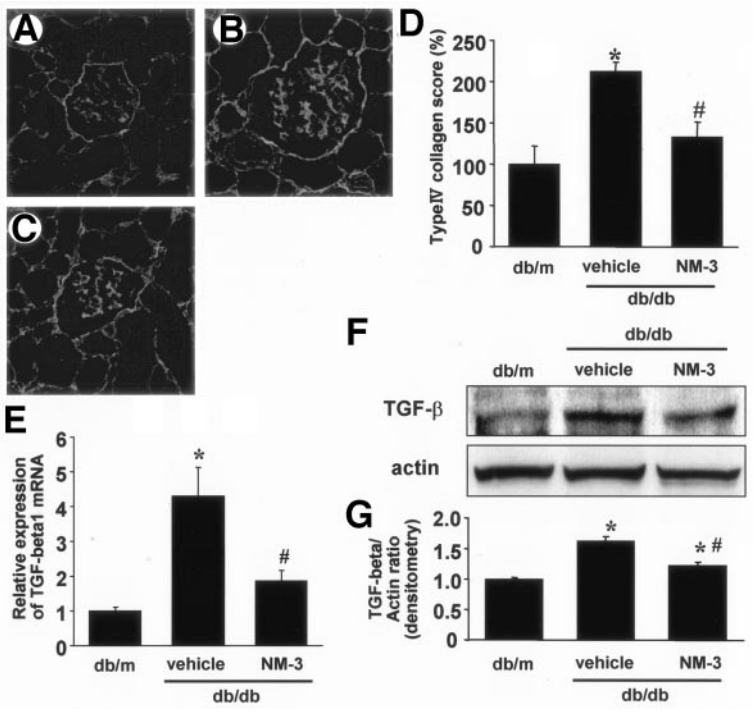

FIG. 3. Glomerular accumulation of type IV collagen was assessed by indirect immunofluorescence method as described in RESEARCH DESIGN AND METHODS for *db/m* mice (*A*), *db/db* mice treated with vehicle buffer (*B*), and *db/db* mice treated with NM-3 (*C*) at 16 weeks of age. *A–C*: Original magnification ×400. *D*: The amount of immunoreactive type IV collagen in glomeruli relative to nondiabetic control *db/m* mice determined by NIH Image is shown; $n = 6$ for each group. Vehicle, *db/db* mice treated with vehicle buffer; NM-3, *db/db* mice treated with NM-3. *$P < 0.001$ vs. *db/m*; #$P < 0.01$ vs. vehicle. *E*: Expression of TGF-β1 mRNA detected by real-time PCR. Total RNA was extracted from kidney cortex and subjected to the examination using quantitative real-time PCR as described in RESEARCH DESIGN AND METHODS. The amount of TGF-β1 mRNA relative to 18s rRNA is shown. Results were expressed relative to *db/m* mice that were arbitrarily assigned a value of 1.0. $n = 5$ for each group. *$P < 0.01$ vs. *db/m*; #$P < 0.05$ vs. vehicle. *F*: Immunoblots for TGF-β and actin are shown. In each lane, 50 mg protein obtained from kidney cortex was loaded. Each band was scanned and subjected to densitometry. *G*: Intensities of TGF-β protein relative to actin are shown. *$P < 0.05$ vs. *db/m*; #$P < 0.005$ vs. vehicle. Each column consists of means ± SE.

resulted in the suppression of diabetes-induced increase of CCr (*db/m* mice, 0.18 ± 0.03 ml/min; *db/db* mice treated with vehicle, 0.45 ± 0.06 ml/min; and *db/db* mice treated with NM-3, 0.27 ± 0.03 ml/min) and UACR (*db/m* mice, 50.0 ± 1.1 μg albumin/mg creatinine; *db/db* mice treated with vehicle, 470.3 ± 20.6 μg albumin/mg creatinine; and *db/db* mice treated with NM-3, 170.4 ± 20.8 μg albumin/mg creatinine, at 8 weeks after initiating treatment). The development of glomerular hyperfiltration and albuminuria in *db/db* mice was significantly suppressed by treatment with NM-3.

Histology and morphometric analysis. Histological examination of the kidneys revealed glomerular hypertrophy and expansion of the mesangial area in vehicle-treated *db/db* mice. After 8 weeks of treatment with NM-3, glomerular hypertrophy and mesangial matrix expansion were significantly inhibited compared with vehicle treatment in *db/db* mice (Fig. 2). Systemic administration of NM-3 did not cause any pathological alterations in liver, lung, or heart of diabetic mice or of nondiabetic mice (data not shown).

Immunohistochemical analysis of glomerular type IV collagen expression. To further evaluate the therapeutic effect of NM-3 in the diabetic nephropathy model, the expression level of type IV collagen was examined by immunofluorescence staining (Fig. 3). The amount of type IV collagen in glomeruli was increased in the vehicle-treated *db/db* mice (Fig. 3*B*) compared with nondiabetic *db/m* mice (Fig. 3*A*). Enhanced immunoreactivity in *db/db* mice was observed mainly in the GBM and mesangial area. Treatment with NM-3 significantly decreased the accumulation of type IV collagen in *db/db* mice (Fig. 3*C* and *D*).

Expression of TGF-β1 mRNA and protein. TGF-β1 is known as a profibrotic growth factor involved in the expansion of mesangial matrix and renal hypertrophy in diabetic nephropathy (34). Vehicle-treated *db/db* mice exhibited increased expression of TGF-β1 mRNA and protein compared with *db/m* mice in the renal cortex. Treatment with NM-3 resulted in the suppression of TGF-β1 mRNA expression in *db/db* mice (Fig. 3*E*). In addition, treatment with NM-3 resulted in the suppression of the increase of renal TGF-β protein levels in *db/db* mice as detected by immunoblot analysis (Fig. 3*F*). These results suggest that NM-3 suppresses the increase of glomerular type IV collagen, mesangial matrix expansion, and renal hypertrophy via, at least in part, downregulating TGF-β1.

Immunohistochemical analysis of glomerular CD31$^+$ endothelial area. We next examined the expression of endothelial cell marker CD31 in glomeruli. In *db/m* mice, CD31 was detected in glomerular capillaries (Fig. 4*A*), and increased expression of CD31 in glomerular capillary area was observed in the vehicle-treated *db/db* mice (Fig. 4*B*). Treatment with NM-3 significantly suppressed the increase of the glomerular CD31$^+$ area in *db/db* mice (Fig. 4*C* and *E*). These results demonstrate that treatment with NM-3 leads to inhibition of increase in the glomerular CD31$^+$ endothelial area in *db/db* mice, possibly via its anti-angiogenic efficacy.

Immunohistochemical analysis of monocyte/macrophage accumulation. We next examined the expression of mouse monocyte/macrophage surface marker F4/80 in glomeruli. In the vehicle-treated *db/db* mice (Fig. 5*B*), the number of F4/80$^+$ cells was significantly increased compared with the *db/m* mice (Fig. 5*A*). Treatment with NM-3 decreased the accumulation of monocyte/macrophage in glomeruli (Fig. 5*C*), suggesting the anti-inflammatory action of NM-3 in this model.

Expression of IL-6 and MCP-1 mRNA. IL-6 and MCP-1 are involved in leukocyte infiltration in association with the development of inflammatory lesions. There were no significant differences in the mRNA levels of these cytokines in renal cortex between the vehicle-treated *db/db* mice and *db/m* mice, as detected by real-time PCR. Treatment with NM-3 failed to affect renal mRNA expression of IL-6 and MCP-1 in *db/db* mice (Fig. 5*E* and *F*), suggesting that the inhibitory effect of NM-3 on monocyte/macrophage recruitment is possibly independent of alterations in the level of these chemokines.

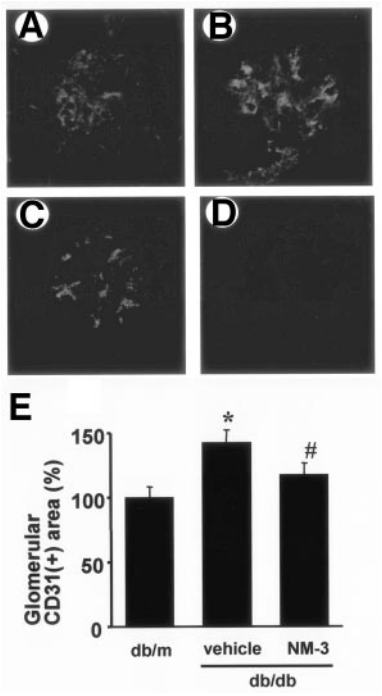

FIG. 4. Immunofluorescent staining of CD31, an endothelial cell marker. Distribution of CD31 was determined by indirect immunofluorescence method as described in RESEARCH DESIGN AND METHODS for *db/m* mice (*A*), *db/db* mice treated with vehicle buffer (*B*), and *db/db* mice treated with NM-3 (*C*) at 16 weeks of age. *D*: No immunoreactivity was observed in sections (*db/db* mice treated with vehicle buffer) incubated with normal IgG in place of primary antibody. *E*: Glomerular CD31$^+$ endothelial area was quantitated as described in RESEARCH DESIGN AND METHODS. Increase in CD31$^+$ glomerular capillary area was significantly suppressed after treatment with NM-3. $n = 6$ for each group. Vehicle, *db/db* mice treated with vehicle buffer; NM-3, *db/db* mice treated with NM-3. *$P < 0.01$ vs. *db/m*; #$P < 0.05$ vs. vehicle. Each column consists of means ± SE.

Protein levels of MCP-1 and TNF-α. The effect of NM-3 on the protein levels of inflammation-associated factors MCP-1 and TNF-α in the renal cortex was studied by immunoblot assay. The level of MCP-1 was significantly increased in vehicle-treated *db/db* mice compared with *db/m* mice (Fig. 5*G* and *H*). Treatment with NM-3 mildly suppressed the increase of MCP-1 in *db/db* mice with statistical significance. The level of TNF-α was increased in *db/db* mice, but there was no difference between NM-3 and vehicle treatment (Fig. 5*G* and *I*).

Expression of VEGF-A, Ang-1, and Ang-2. The effect of NM-3 on the expression of angiogenesis-associated factors VEGF-A, Ang-1, and Ang-2 in the renal cortex was studied by immunoblot assay. The levels of VEGF-A and Ang-2 were significantly increased in vehicle-treated *db/db* mice compared with *db/m* mice (Fig. 6*B* and *D*). Treatment with NM-3 significantly suppressed the increase of VEGF-A and Ang-2 in *db/db* mice. The level of Ang-1 was detected in *db/m* mice but was not significantly altered in vehicle- or NM-3–treated *db/db* mice (Fig. 6*C*).

Immunohistochemical analysis of VEGF-A. We next examined the expression of VEGF-A in glomeruli by indirect immunohistochemistry. In vehicle-treated *db/db* mice, immunoreactivity for VEGF-A was increased compared with *db/m* mice, mainly localized to podocytes (Fig. 6*E–G*). Treatment with NM-3 resulted in decreased immunoreactivity for VEGF-A in glomeruli compared with vehicle-treated *db/db* mice.

Expression of nephrin mRNA and protein. The expression of nephrin, an essential component of the slit-diaphragm involved in the regulation of the glomerular filtration barrier, was studied using real-time PCR and immunoblot assay. Vehicle buffer–treated *db/db* mice exhibited reduced renal expression levels of nephrin mRNA and protein compared with *db/m* mice. Treatment with NM-3 resulted in the recovery of nephrin mRNA and protein expression (Fig. 7). These results suggest the supportive role of NM-3 in maintaining nephrin and thus the glomerular filtration barrier possibly associated with the suppression of albuminuria in *db/db* mice.

Protein expression of TGF-β in cultured mouse mesangial cells. To further clarify the mechanism of action of NM-3 in suppressing the increase of TGF-β in diabetic mice, we performed cell culture analysis using primary mouse mesangial cells. In a preliminary study, the protein level of TGF-β in mesangial cells was significantly increased at 48 h after incubation in medium supplemented with 25 mmol/l glucose compared with incubation for the same time interval under normal glucose conditions (immunoblot). Therefore, mesangial cells were incubated for 48 h under normal or high glucose conditions in the following experiments. Addition of mannitol to culture condition under normal glucose did not lead to the increase of TGF-β, thus excluding the potential effect by elevated osmotic pressure. Treatment with NM-3 resulted in the suppression of the increase of TGF-β protein induced by high glucose in a dose-dependent manner (Fig. 8*A* and *C*). These results demonstrate the direct action of NM-3 on mesangial cells in suppressing upregulation of TGF-β induced by high glucose.

Expression of VEGF-A protein in cultured mouse mesangial cells and podocytes. To further clarify the mechanism of action of NM-3 in suppressing the increase of VEGF-A in diabetic mice, we performed cell culture analysis using primary mouse mesangial cells and mouse podocytes. In a preliminary study, the protein level of VEGF-A in mesangial cells and podocytes was significantly increased at 48 h after incubating in medium supplemented with 25 mmol/l glucose compared with incubation for the same time interval under normal glucose conditions (immunoblot). Therefore, cells were incubated for 48 h under normal or high glucose conditions in the following experiments. We did not observe apparent morphological alterations suggestive of cytotoxicity by treatment with NM-3 under different concentrations (1–100 mg/ml) in mesangial cells and podocytes. Incubation of cells in medium containing normal glucose concentration supplemented with mannitol failed to present any differences in the levels of TGF-β or VEGF compared with normal glucose alone, indicating the induction of these proteins by high glucose independent of hyperosmolarity. Treatment with NM-3 resulted in the suppression of the increase of VEGF protein induced by high glucose in a dose-dependent manner in both mesangial cells and podocytes (Fig. 8*A*, *B*, *D*, and *E*). These results demonstrate the direct action of NM-3 on mesangial cells and podocytes in suppressing upregulation of VEGF-A induced by high glucose condition.

DISCUSSION

Diabetic nephropathy is the major underlying cause of ESRD, and appropriate management of blood glucose and blood pressure is known to be important in preventing the

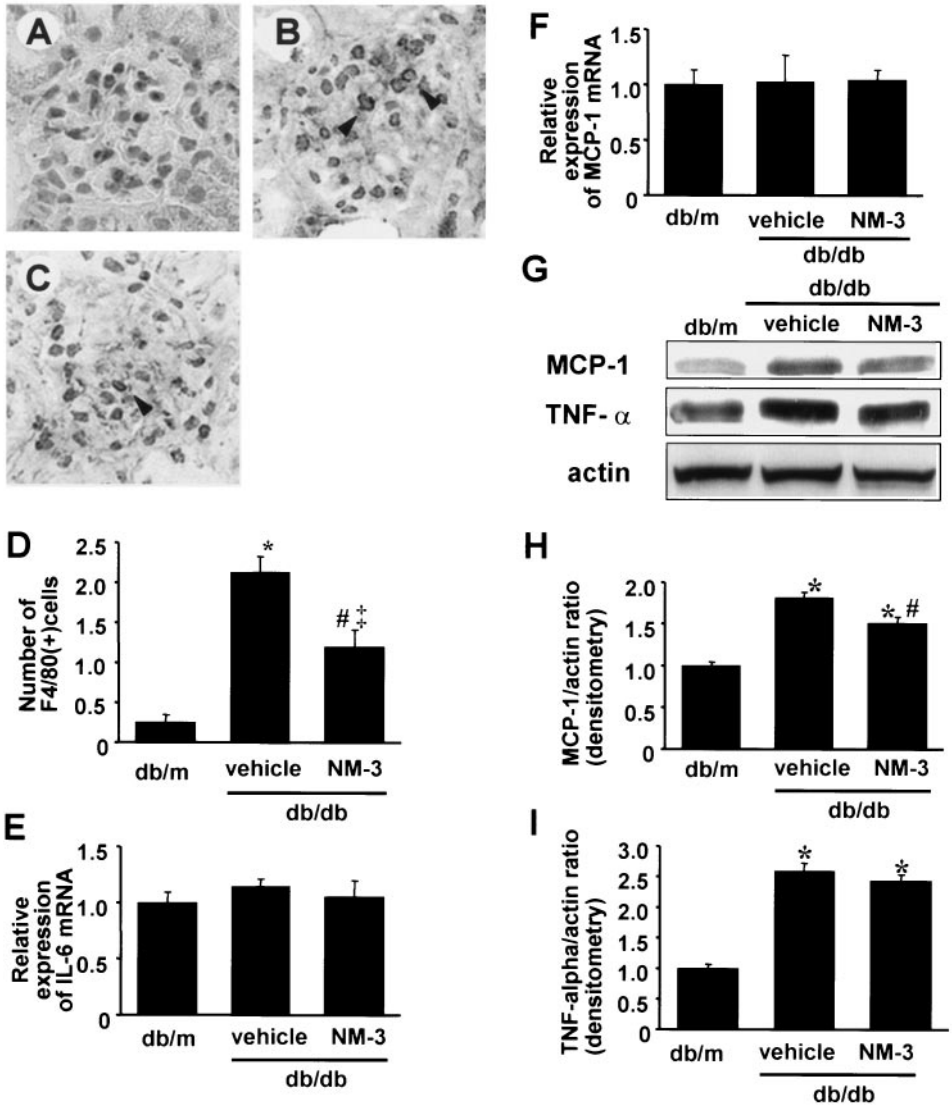

FIG. 5. Immunohistochemistry of F4/80$^+$ monocyte/macrophage. Distribution of F4/80$^+$ cells was determined by indirect immunohistochemistry for *db/m* mice (*A*), *db/db* mice treated with vehicle buffer (*B*), and *db/db* mice treated with NM-3 (*C*) at 16 weeks of age. F4/80$^+$ cells were observed in diabetic mice (arrowheads) and in diabetic mice treated with NM-3 to a lesser extent. Representative light microscopic appearance of glomerulus is shown (original magnification ×400). *D*: The number of glomerular F4/80$^+$ monocyte/macrophage is shown. Increase in F4/80$^+$ monocyte/macrophage number was significantly suppressed after treatment with NM-3; $n = 6$ for each group. Vehicle, *db/db* mice treated with vehicle buffer; NM-3, *db/db* mice treated with NM-3. *$P < 0.001$ vs. *db/m*; #$P < 0.01$ vs. vehicle; ‡$P < 0.01$ vs. *db/m*. *E*: Expression of IL-6 mRNA detected by real-time PCR. Total RNA was extracted from kidney cortex and subjected to quantitative real-time PCR. The amount of IL-6 mRNA relative to 18s rRNA is shown. Results were expressed relative to *db/m* mice that were arbitrarily assigned a value of 1.0. $n = 5$ for each group. *F*: Expression of MCP-1 mRNA detected by real-time PCR. The amount of MCP-1 mRNA relative to 18s rRNA is shown. Results were expressed relative to *db/m* mice that were arbitrarily assigned a value of 1.0. $n = 5$ for each group. *G*: Immunoblots for MCP-1, TNF-α, and actin are shown. In each lane, 50 μg protein obtained from kidney cortex was loaded. Each band was scanned and subjected to densitometry. *H*: Intensities of MCP-1 protein relative to actin are shown. *$P < 0.005$ vs. *db/m*; #$P < 0.05$ vs. vehicle. *I*: Intensities of TNF-α protein relative to actin are shown. *$P < 0.001$ vs. *db/m*. Vehicle, *db/db* mice treated with vehicle buffer; NM-3, *db/db* mice treated with NM-3. $n = 5$ for each group. Each column consists of means ± SE.

progression. Although clinical trials revealed the beneficial effect of angiotensin type 1 receptor blockade in preventing the progression of diabetic nephropathy, novel and distinct therapeutic approaches are required, considering the vast and increasing population of diabetic nephropathy.

Angiogenesis is regulated by the balance between proangiogenic factors and antiangiogenic factors (3,35,36). The involvement of VEGF-A in progressing diabetic nephropathy has been demonstrated in a number of previous reports suggesting the therapeutic potential of the inhibition of VEGF-A signaling (6,7,9,10,37). We recently reported that the renal expression of VEGF and Ang-2 was increased in a streptozotocin-induced type 1 diabetic mouse model. Antiangiogenic tumstatin peptide and endostatin peptide inhibited the increase of VEGF and Ang-2, potentially associated with the observed therapeutic effects in early diabetic nephropathy (15,16), suggesting the involvement of these angiogenesis-associated factors in the progression of diabetic nephropathy.

Cytogenin is a natural product of microbial origin possessing the potent antiarthritic effects against type II collagen–induced arthritis (38) and antiangiogenic activity in a mouse dorsal air sac assay model (20). Whereas cytogenin is biologically instable with limited therapeutic effects, NM-3, a derivative of cytogenin, is considerably orally bioavailable and biologically stable (39). NM-3 was also revealed to possess potent therapeutic effects on the type II collagen–induced arthritis (40) and antiangiogenic activity in the mouse dorsal air sac model (21). Furthermore, in vitro proliferation of endothelial cells was inhibited by NM-3 at concentrations 10-fold less than those required to inhibit normal fibroblasts or tumor cells (26), suggesting its potent direct antiangiogenic action on endothelial cells.

In the present study, we used *db/db* mice, a model of obese type 2 diabetes, to demonstrate the potential therapeutic efficacy of NM-3 in diabetic nephropathy. The *db/db* mouse is characterized by obesity, sustained hyperglycemia, hyperinsulinemia, and lack of ketonuria due to the defect of leptin receptor in the hypothalamus accompanied by the typical diabetic renal alterations characterized by renal/glomerular hypertrophy, thickening of GBM, albuminuria, and mesangial matrix accumulation within 2 months of onset of diabetes (25,41,42).

Administration of NM-3 did not affect blood glucose, body weight, food consumption, and serum insulin concentration in *db/db* mice. In addition, treatment with NM-3 did not give rise to any pathological alterations in heart or

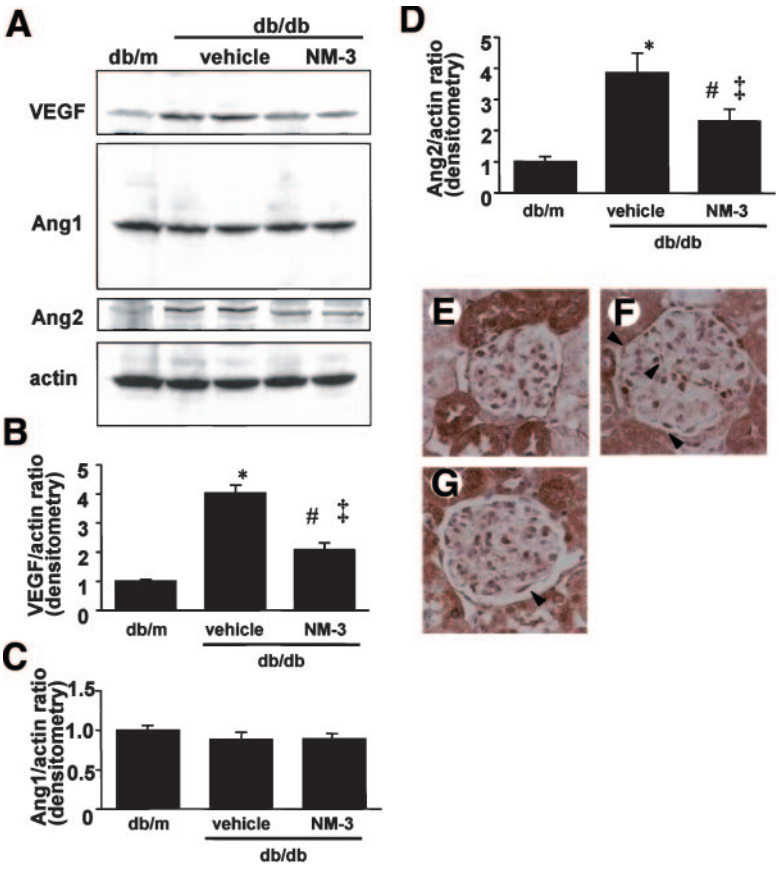

FIG. 6. ***A–D*****: Immunoblot analysis.** ***A*****: Immunoblots for VEGF-A, Ang-1, Ang-2, and actin are shown. In each lane, 50 μg protein obtained from kidney cortex was loaded. Each band was scanned and subjected to densitometry.** ***B*****: Intensities of VEGF-A protein relative to actin are shown. *P < 0.02 vs. *db/m*; #P < 0.05 vs. vehicle; ‡P < 0.05 vs. *db/m*.** ***C*****: Intensities of Ang-1 protein relative to actin are shown.** ***D*****: Intensities of Ang-2 protein relative to actin are shown. *P < 0.05 vs. *db/m*; #P < 0.05 vs. vehicle; ‡P < 0.05 vs. *db/m*. Vehicle, *db/db* mice treated with vehicle buffer; NM-3, *db/db* mice treated with NM-3. n = 5 for each group.** ***E–G*****: Immunohistochemistry of VEGF-A. Distribution of VEGF-A was examined by indirect immunohistochemistry for *db/m* mice (*E*), *db/db* mice treated with vehicle buffer (*F*), and *db/db* mice treated with NM-3 (*G*) at 16 weeks of age.** ***F*****: Increased immunoreactivity for VEGF-A was mainly localized to glomerular podocytes (arrowheads) in vehicle-treated diabetic mice.** ***G*****: Immunoreactivity for VEGF-A was observed to a lesser extent in diabetic mice treated with NM-3.**

liver and failed to affect wound repair (data not shown). Previous reports described inconsistent results on CCr within 2 months after the onset of diabetes in *db/db* mice (10,25). The discrepant outcomes may be attributed to a variable susceptibility to diabetes in subbreedings of the *db/db* mouse strain. In the present study, we observed increased CCr and albuminuria at this time point in vehicle-treated *db/db* mice. Renal alterations such as increased urinary albumin excretion, glomerular hypertrophy, glomerular hyperfiltration, and the increase of mesangial matrix were significantly inhibited by NM-3 at 8 weeks after starting treatment (16 weeks of age). Renal hypertrophy observed in *db/db* mice tended to be slightly decreased by NM-3. Considering the dominant contribution of the tubular compartment in organizing renal mass, we speculate that NM-3 might have mainly regulated glomerular hypertrophy observed in diabetic nephropathy, thus not leading to remarkable effects on renal hypertrophy.

The accumulation of type IV collagen in glomeruli in *db/db* mice was also inhibited by NM-3, potentially associated with the suppression of renal TGF-β1 mRNA levels. Connective tissue growth factor mediates the effect of TGF-β in inducing mesangial matrix expansion and mesangial cell hypertrophy in diabetic nephropathy (43). The role of VEGF-A in inducing the expression of connective tissue growth factor in retinal capillary cells in association with the development of retinal neovascular diseases has been reported (44). In addition, podocyte-derived VEGF-A induced by TGF-β1 was reported to stimulate the production of α3(IV) collagen, a component of α-chains in GBM (45). Therefore, the inhibitory effect of NM-3 on the increase of glomerular type IV collagen and mesangial matrix expansion may, at least in part, be mediated via downregulation of VEGF-A, which presumably is involved in mediating the profibrotic effect of TGF-β1 in diabetic nephropathy. It has been reported that expression of TGF-β is increased in mesangial cells cultured under high glucose conditions (46). To determine the potential direct effect of NM-3 on the synthesis of TGF-β in mesangial cells induced by hyperglycemia, we performed in vitro experiments and observed inhibitory effects of NM-3 on high glucose–induced increase of TGF-β in cultured mouse mesangial cells.

Treatment with NM-3 suppressed the increase of the $CD31^+$ glomerular endothelial area in *db/db* mice, potentially due to the antiangiogenic activity of NM-3 in association with the suppression of VEGF. Increased accumulation of monocytes/macrophages in glomeruli has been reported in type 1 diabetic (15) and *db/db* mouse models (47). IL-6 and MCP-1 induce the recruitment of monocyte/macrophage, and MCP-1 especially is involved in the development of diabetic nephropathy (48). In the present study, the mRNA expression of IL-6 and MCP-1 did not alter in *db/db* mice, and NM-3 did not affect either. The protein level of MCP-1 was partially suppressed by treatment with NM-3 with statistical significance as detected by immunoblot, suggesting its regulatory role on MCP-1 via posttranscriptional regulation. The protein level of TNF-α, another inflammatory cytokine involved in various inflammation processes and the development of diabetic nephropathy, was not altered by treatment with NM-3. VEGF-A promotes vascular permeability and also mediates recruitment of monocyte/macrophage in a receptor-dependent fashion (49). Therefore, the observed increase of monocyte/macrophage accumulation in *db/db* mice was possibly mediated via stimulation of VEGF-A, and the inhibitory effect of NM-3 on the recruitment of monocytes/macrophages may result from interference with the

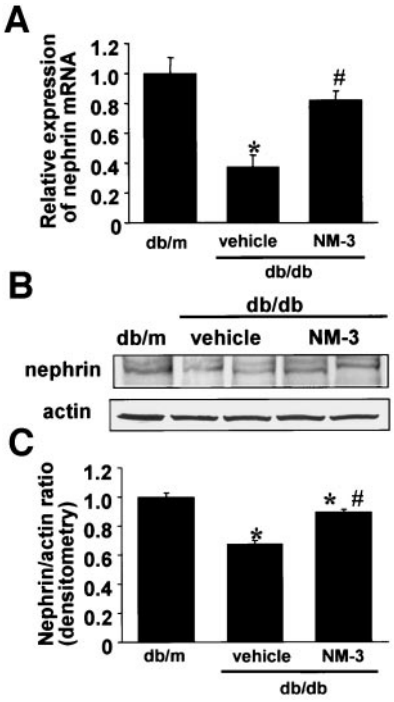

FIG. 7. ***A*****: Expression of nephrin mRNA detected by real-time PCR. Total RNA was extracted from kidney cortex and subjected to quantitative real-time PCR as described in RESEARCH DESIGN AND METHODS. The amount of nephrin mRNA relative to 18s rRNA is shown. Results were expressed relative to *db/m* mice that were arbitrarily assigned a value of 1.0. Vehicle, *db/db* mice treated with vehicle buffer; NM-3, *db/db* mice treated with NM-3. $n = 5$ for each group. *$P < 0.005$ vs. *db/m*; #$P < 0.01$ vs. vehicle. *B* and *C*: Immunoblot analysis of nephrin. *B*: Immunoblots for nephrin and actin are shown. In each lane, 50 μg protein obtained from kidney cortex was loaded. Each band was scanned and subjected to densitometry. *C*: Intensities of nephrin protein relative to actin are shown. *$P < 0.05$ vs. *db/m*; #$P < 0.001$ vs. vehicle. $n = 5$ for each group. Each column consists of means ± SE.**

VEGF-A signaling by NM-3, in addition to its inhibitory effect on the protein level of MCP-1.

We next examined the effect of NM-3 on the renal level of angiogenesis-associated factors. A previous report demonstrated the increased VEGF expression mainly on podocytes in *db/db* mice by 13 weeks and even at 27 weeks of age (8). Consistent with this previous report, the level of VEGF-A was increased in the renal cortex of *db/db* mice in the present study at 16 weeks of age. Treatment with NM-3 significantly suppressed the increase of VEGF-A in the renal cortex of *db/db* mice. The therapeutic effect of NM-3 in diabetic nephropathy may be attributed, at least in part, to the inhibition of the VEGF-A pathway in analogy with previous studies using neutralizing anti–VEGF-A antibodies (9,10). A previous report described podocyte-specific localization of VEGF in *db/db* mice (8), which is consistent with our immunohistochemical findings for VEGF. Inhibitory effect by NM-3 on immunoreactivity for VEGF in podocytes was also observed. In addition to production of VEGF by cultured podocytes in response to high glucose (50), the increase of VEGF protein synthesis was also observed in mesangial cells cultured under a high ambient glucose conditions (51). To examine the potential direct effect of NM-3 on the synthesis of VEGF induced by high glucose in mesangial cells and podocytes, we next performed cell culture experiments. Inhibitory effect of NM-3 on high glucose–induced upregulation of VEGF was observed in both cultured mouse mesangial cells and podocytes in a dose-dependent manner. Treatment with high concentrations of NM-3 did not exhibit apparent morphological changes suggestive of cytotoxicity in both cell types. Our results demonstrate the direct suppressive effect of NM-3 on VEGF expression in mesangial cells and podocytes under high glucose condition, in addition to its known effects on endothelial cells.

In regard to Angs, the expression of Ang-1 in the renal cortex was not altered in *db/db* mice, in line with our

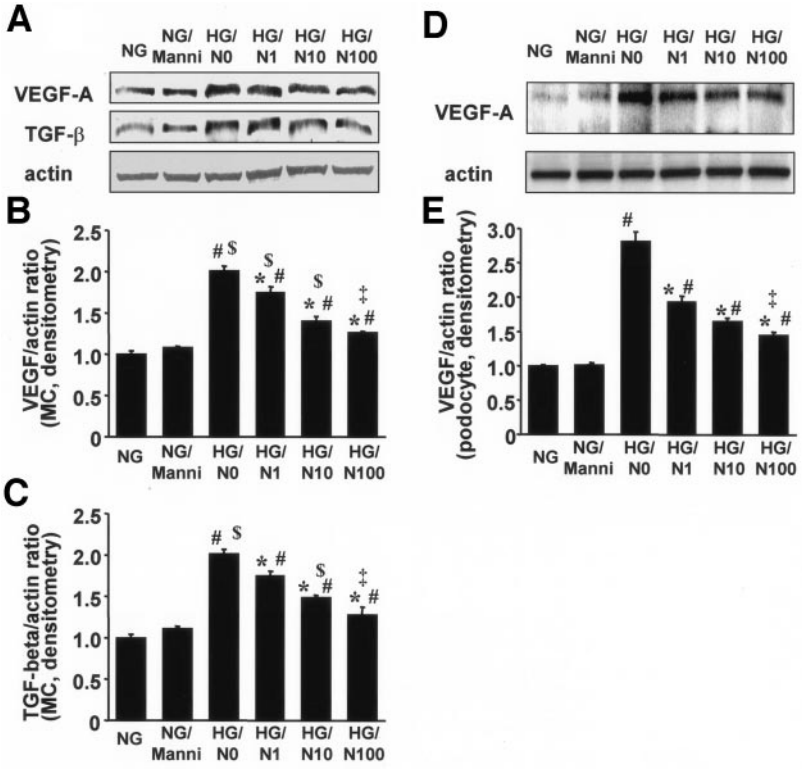

FIG. 8. ***A–E*****: Immunoblot analysis. *A*: Immunoblots for VEGF-A, TGF-β, and actin are shown. In each lane, 20 mg protein obtained from mouse mesangial cells was loaded. Each band was scanned and subjected to densitometry. *B*: Intensities of VEGF-A protein relative to actin are shown. *$P < 0.05$ vs. NG/N0; #$P < 0.001$ vs. NG; ‡$P < 0.001$ vs. HG/N1. $$P < 0.001$ vs. NG/Manni. *C*: Intensities of TGF-β protein relative to actin are shown. *$P < 0.005$ vs. HG/N0; #$P < 0.001$ vs. NG; ‡$P < 0.001$ vs. HG/N1; $$P < 0.001$ vs. NG/Manni. *D*: Immunoblots for VEGF-A and actin are shown. In each lane, 20 μg protein obtained from mouse podocyte culture was loaded. Each band was scanned and subjected to densitometry. *E*: Intensities of VEGF-A protein relative to actin are shown. *$P < 0.005$ vs. HG/N0; #$P < 0.05$ vs. NG or NG/Manni; ‡$P < 0.005$ vs. HG/N1. $n = 5$ for each group. Each column consists of means ± SE. MC, mesangial cells; NG, normal D-glucose (5.5 mmol/l); NG/Manni, normal D-glucose plus D-mannitol (19.5 mmol/l); HG/N0, high D-glucose (25 mmol/l); HG/N1, high D-glucose plus 1 mg/ml NM-3; HG/N10, high D-glucose plus 10 mg/ml NM-3; HG/N100, high D-glucose plus 100 mg/ml NM-3.**

previous observation in type 1 diabetic mouse model (15,16). Treatment with NM-3 failed to affect the level of renal Ang-1. In contrast, the expression of Ang-2 was markedly increased in *db/db* mice, which is similar to our previous results in type 1 diabetic mouse model (15,16). Treatment with NM-3 significantly suppressed the increase of Ang-2 in renal cortex of *db/db* mice. The marked increase of Ang-2 over Ang-1 in *db/db* mice suggests the proangiogenic milieu considering simultaneous upregulation of VEGF-A and the "leaky " condition of capillaries in association with increased monocyte recruitment.

Among various podocyte proteins composing slit diaphragm, we investigated alteration in the levels of nephrin, a functional molecule of the interpodocyte filtration slit diaphragm. Altered expression of nephrin has been reported in the setting of diabetic nephropathy (17,18, 37,52). Reduction in both mRNA and protein expression of nephrin was associated with proteinuria in diabetic spontaneously hypertensive rats (52). In human diabetic nephropathy, reduced mRNA and protein expression of nephrin was demonstrated (17,18). A recent report describes reduced expression of nephrin in *db/db* mouse kidney (53). In the present study, we observed decreased mRNA and protein expression of nephrin in *db/db* mice, which is consistent with previous observations from our laboratory and others (15,16,53). Administration of NM-3 resulted in significant recovery of nephrin in *db/db* mice. Considering the pivotal role of nephrin in the maintenance of the glomerular filtration barrier, the recovery of nephrin by treatment with NM-3 may be associated with decreased albuminuria. The indirect influence of glomerular endothelial cells toward podocytes possibly mediated via secreted factors or alteration on a matrix microenvironment may explain the observed effect of NM-3 on nephrin levels. A genetic study using mice with podocyte-specific overexpression or deletion of VEGF-A suggested the importance of an appropriate level of VEGF-A in maintaining a proper glomerular filtration barrier (54). The role of Ang-1 in maintaining glomerular endothelium and regulating the action of VEGF-A on glomerular permselectivity (55) further demonstrates that the interaction between glomerular endothelial cells and podocytes is involved in maintaining proper glomerular structures as well as biological functions. The direct effect of NM-3 on podocytes leading to the restoration of nephrin needs further investigation. A recent report describes lower mRNA expression of other podocyte proteins such as CD2AP and actinin-4 in microalbuminuric patients compared with normoalbuminuric patients of type 2 diabetes (56), and alteration of the expression of these other podocyte proteins in the present experimental groups also need to be investigated in future.

In the present study, we treated *db/db* mice with systemic administration of antiangiogenic NM-3. Although no adverse effects were observed in NM-3–treated diabetic mice, which is consistent with the results from a recent phase I clinical trial of NM-3 showing no dose-limiting toxicities (24,57), it is possible that systemic administration of antiangiogenic reagents may suppress angiogenic response in a setting requiring angiogenic neovessel formation, such as peripheral neuropathy, nonhealing ulcers, and limb ischemia, pathological conditions complicated in patients with advanced diabetes. Because we attempted to observe the therapeutic effects of NM-3 in a relatively early stage of diabetic nephropathy before the incidence of apparent renal dysfunction, further assessment by the administration of NM-3 for an extended period of time may address these issues.

In conclusion, we demonstrated here that the administration of antiangiogenic NM-3 significantly ameliorated renal alterations in obese type 2 diabetic mice, in addition to its known therapeutic effects on solid tumors (22,23,26) and rheumatoid arthritis (40). Considering its high oral bioavailability and excellent safety profile demonstrated by the phase I clinical trials in patients with cancers, our results convincingly indicate the potential of NM-3 for application into clinic to prevent the progression of diabetic nephropathy alone or in combination with known therapeutic approaches.

ACKNOWLEDGMENTS

Y.M. has received a research grant from a grant-in-aid for Scientific Research from the Ministry of Education, Science, and Culture of Japan and grants-in-aid from the Tokyo Biochemical Research Foundation, the Inamori Foundation, and the Suzuken Memorial Foundation. Y.M. is a recipient of the 2003 Research Award from the Kobayashi Magobei Memorial Foundation for Medical Science, the 2003 Research Award from the Ryobi Teien Memorial Foundation, the 2004 Research Award from the Sanyo Broadcast Academic and Cultural Foundation, and the 2005 Oshima Award (Young Investigator Award) from the Japanese Society of Nephrology.

We appreciate Dr. Peter Mundel and Dr. Jun Wada (Okayama University Graduate School of Medicine, Dentistry and Pharmaceutical Sciences, Okayama, Japan) for providing cultured podocytes and mesangial cells. We also appreciate Dr. Tatsuo Okada (Okayama University Graduate School of Medicine, Dentistry and Pharmaceutical Sciences, Okayama, Japan) for technical assistance in cell culture experiments.

REFERENCES

1. Makino H, Kashihara N, Sugiyama H, Kanao K, Sekikawa T, Okamoto K, Maeshima Y, Ota Z, Nagai R: Phenotypic modulation of the mesangium reflected by contractile proteins in diabetes. *Diabetes* 45:488–495, 1996
2. Sharma K, Ziyadeh FN: Hyperglycemia and diabetic kidney disease: the case for transforming growth factor-β as a key mediator. *Diabetes* 44: 1139–1146, 1995
3. Folkman J: Angiogenesis in cancer, vascular, rheumatoid and other disease. *Nat Med* 1:27–31, 1995
4. Ferrara N: Vascular endothelial growth factor and the regulation of angiogenesis. *Recent Prog Horm Res* 55:15–35, 2000
5. Dvorak HF, Brown LF, Detmar M, Dvorak AM: Vascular permeability factor/vascular endothelial growth factor, microvascular hyperpermeability, and angiogenesis. *Am J Pathol* 146:1029–1039, 1995
6. Cooper ME, Vranes D, Youssef S, Stacker SA, Cox AJ, Rizkalla B, Casley DJ, Bach LA, Kelly DJ, Gilbert RE: Increased renal expression of vascular endothelial growth factor (VEGF) and its receptor VEGFR-2 in experimental diabetes. *Diabetes* 48:2229–2239, 1999
7. Tsuchida K, Makita Z, Yamagishi S, Atsumi T, Miyoshi H, Obara S, Ishida M, Ishikawa S, Yasumura K, Koike T: Suppression of transforming growth factor beta and vascular endothelial growth factor in diabetic nephropathy in rats by a novel advanced glycation end product inhibitor, OPB-9195. *Diabetologia* 42:579–588, 1999
8. Wendt TM, Tanji N, Guo J, Kislinger TR, Qu W, Lu Y, Bucciarelli LG, Rong LL, Moser B, Markowitz GS, Stein G, Bierhaus A, Liliensiek B, Arnold B, Nawroth PP, Stern DM, D'Agati VD, Schmidt AM: RAGE drives the development of glomerulosclerosis and implicates podocyte activation in the pathogenesis of diabetic nephropathy. *Am J Pathol* 162:1123–1137, 2003
9. de Vriese AS, Tilton RG, Elger M, Stephan CC, Kriz W, Lameire NH: Antibodies against vascular endothelial growth factor improve early renal dysfunction in experimental diabetes. *J Am Soc Nephrol* 12:993–1000, 2001

10. Flyvbjerg A, Dagnaes-Hansen F, De Vriese AS, Schrijvers BF, Tilton RG, Rasch R: Amelioration of long-term renal changes in obese type 2 diabetic mice by a neutralizing vascular endothelial growth factor antibody. *Diabetes* 51:3090–3094, 2002
11. Suri C, Jones PF, Patan S, Bartunkova S, Maisonpierre PC, Davis S, Sato TN, Yancopoulos GD: Requisite role of angiopoietin-1, a ligand for the TIE2 receptor, during embryonic angiogenesis. *Cell* 87:1171–1180, 1996
12. Maisonpierre PC, Suri C, Jones PF, Bartunkova S, Wiegand SJ, Radziejewski C, Compton D, McClain J, Aldrich TH, Papadopoulos N, Daly TJ, Davis S, Sato TN, Yancopoulos GD: Angiopoietin-2, a natural antagonist for Tie2 that disrupts in vivo angiogenesis. *Science* 277:55–60, 1997
13. Visconti RP, Richardson CD, Sato TN: Orchestration of angiogenesis and arteriovenous contribution by angiopoietins and vascular endothelial growth factor (VEGF). *Proc Natl Acad Sci U S A* 99:8219–8224, 2002
14. Woolf AS, Yuan HT: Angiopoietin growth factors and Tie receptor tyrosine kinases in renal vascular development. *Pediatr Nephrol* 16:177–184, 2001
15. Yamamoto Y, Maeshima Y, Kitayama H, Kitamura S, Takazawa Y, Sugiyama H, Yamasaki Y, Makino H: Tumstatin peptide, an inhibitor of angiogenesis, prevents glomerular hypertrophy in the early stage of diabetic nephropathy. *Diabetes* 53:1831–1840, 2004
16. Ichinose K, Maeshima Y, Yamamoto Y, Kitayama H, Takazawa Y, Hirokoshi K, Sugiyama H, Yamasaki Y, Eguchi K, Makino H: Anti-angiogenic endostatin peptide ameliorates renal alterations in the early stage of type 1 diabetic nephropathy model. *Diabetes* 54:2891–2903, 2005
17. Doublier S, Salvidio G, Lupia E, Ruotsalainen V, Verzola D, Deferrari G, Camussi G: Nephrin expression is reduced in human diabetic nephropathy: evidence for a distinct role for glycated albumin and angiotensin II. *Diabetes* 52:1023–1030, 2003
18. Benigni A, Gagliardini E, Tomasoni S, Abbate M, Ruggenenti P, Kalluri R, Remuzzi G: Selective impairment of gene expression and assembly of nephrin in human diabetic nephropathy. *Kidney Int* 65:2193–2200, 2004
19. Nyengaard JR, Rasch R: The impact of experimental diabetes mellitus in rats on glomerular capillary number and sizes. *Diabetologia* 36:189–194, 1993
20. Oikawa T, Sasaki M, Inose M, Shimamura M, Kuboki H, Hirano S, Kumagai H, Ishizuka M, Takeuchi T: Effects of cytogenin, a novel microbial product, on embryonic and tumor cell-induced angiogenic responses in vivo. *Anticancer Res* 17:1881–1886, 1997
21. Nakashima T, Hirano S, Agata N, Kumagai H, Isshiki K, Yoshioka T, Ishizuka M, Maeda K, Takeuchi T: Inhibition of angiogenesis by a new isocoumarin, NM-3. *J Antibiot* (*Tokyo*) 52:426–428, 1999
22. Reimer CL, Agata N, Tammam JG, Bamberg M, Dickerson WM, Kamphaus GD, Rook SL, Milhollen M, Fram R, Kalluri R, Kufe D, Kharbanda S: Antineoplastic effects of chemotherapeutic agents are potentiated by NM-3, an inhibitor of angiogenesis. *Cancer Res* 62:789–795, 2002
23. Agata N, Nogi H, Bamberg M, Milhollen M, Pu M, Weitman S, Kharbanda S, Kufe D: The angiogenesis inhibitor NM-3 is active against human NSCLC xenografts alone and in combination with docetaxel. *Cancer Chemother Pharmacol* 56:610–614, 2005
24. Agata N, Nogi H, Milhollen M, Kharbanda S, Kufe D: 2-(8-Hydroxy-6-methoxy-1-oxo-1H-2-benzopyran-3-yl)propionic acid, a small molecule isocoumarin, potentiates dexamethasone-induced apoptosis of human multiple myeloma cells. *Cancer Res* 64:8512–8516, 2004
25. Cohen MP, Clements RS, Cohen JA, Shearman CW: Prevention of decline in renal function in the diabetic db/db mouse. *Diabetologia* 39:270–274, 1996
26. Salloum RM, Jaskowiak NT, Mauceri HJ, Seetharam S, Beckett MA, Koons AM, Hari DM, Gupta VK, Reimer C, Kalluri R, Posner MC, Hellman S, Kufe DW, Weichselbaum RR: NM-3, an isocoumarin, increases the antitumor effects of radiotherapy without toxicity. *Cancer Res* 60:6958–6963, 2000
27. Maeshima Y, Kashihara N, Yasuda T, Sugiyama H, Sekikawa T, Okamoto K, Kanao K, Watanabe Y, Kanwar YS, Makino H: Inhibition of mesangial cell proliferation by E2F decoy oligodeoxynucleotide in vitro and in vivo. *J Clin Invest* 101:2589–2597, 1998
28. Takazawa Y, Maeshima Y, Kitayama H, Yamamoto Y, Kawachi H, Shimizu F, Matsui H, Sugiyama H, Yamasaki Y, Makino H: Infusion of angiotensin II reduces loss of glomerular capillary area in the early phase of anti-Thy-1.1 nephritis possibly via regulating angiogenesis-associated factors. *Kidney Int* 68:704–722, 2005
29. Maeshima Y, Colorado PC, Torre A, Holthaus KA, Grunkemeyer JA, Ericksen MB, Hopfer H, Xiao Y, Stillman IE, Kalluri R: Distinct antitumor properties of a type IV collagen domain derived from basement membrane. *J Biol Chem* 275:21340–21348, 2000
30. Maeshima Y, Manfredi M, Reimer C, Holthaus KA, Hopfer H, Chandamuri BR, Kharbanda S, Kalluri R: Identification of the antiangiogenic site within vascular basement membrane-derived tumstatin. *J Biol Chem* 276:15240–15248, 2001
31. Maeshima Y, Sudhakar A, Lively JC, Ueki K, Kharbanda S, Kahn CR, Sonenberg N, Hynes RO, Kalluri R: Tumstatin, an endothelial cell-specific inhibitor of protein synthesis. *Science* 295:140–143, 2002
32. Mundel P, Reiser J, Zuniga Mejia Borja A, Pavenstadt H, Davidson GR, Kriz W, Zeller R: Rearrangements of the cytoskeleton and cell contacts induce process formation during differentiation of conditionally immortalized mouse podocyte cell lines. *Exp Cell Res* 236:248–258, 1997
33. Baba M, Wada J, Eguchi J, Hashimoto I, Okada T, Yasuhara A, Shikata K, Kanwar YS, Makino H: Galectin-9 inhibits glomerular hypertrophy in db/db diabetic mice via cell-cycle-dependent mechanisms. *J Am Soc Nephrol* 16:3222–3234, 2005
34. Sharma K, Jin Y, Guo J, Ziyadeh FN: Neutralization of TGF-β by anti-TGF-β antibody attenuates kidney hypertrophy and the enhanced extracellular matrix gene expression in STZ-induced diabetic mice. *Diabetes* 45:522–530, 1996
35. Maeshima Y, Yerramalla UL, Dhanabal M, Holthaus KA, Barbashov S, Kharbanda S, Reimer C, Manfredi M, Dickerson WM, Kalluri R: Extracellular matrix-derived peptide binds to alpha(v)beta(3) integrin and inhibits angiogenesis. *J Biol Chem* 276:31959–31968, 2001
36. Kalluri R: Basement membranes: structure, assembly and role in tumour angiogenesis. *Nat Rev Cancer* 3:422–433, 2003
37. Wolf G, Chen S, Ziyadeh FN: From the periphery of the glomerular capillary wall toward the center of disease: podocyte injury comes of age in diabetic nephropathy. *Diabetes* 54:1626–1634, 2005
38. Hirano S, Wakazono K, Agata N, Mase T, Yamamoto R, Matsufuji M, Sakata N, Iguchi H, Tone H, Ishizuka M, et al.: Effects of cytogenin, a novel anti-arthritic agent, on type II collagen-induced arthritis in DBA/1J mice and adjuvant arthritis in Lewis rats. *Int J Tissue React* 16:155–162, 1994
39. Matsumoto N, Nakashima T, Isshiki K, Kuboki H, Hirano SI, Kumagai H, Yoshioka T, Ishizuka M, Takeuchi T: Synthesis and biological evaluation of cytogenin derivatives. *J Antibiot* (*Tokyo*) 54:285–296, 2001
40. Agata N, Hirano S, Abe C, Nakashima T, Tsuchiya A, Kumagai H, Isshiki K, Yoshioka T, Ishizuka M, Takeuchi T: Suppression of type II collagen-induced arthritis by a new isocoumarin, NM-3. *Res Commun Mol Pathol Pharmacol* 108:297–309, 2000
41. Koenig RJ, Cerami A: Synthesis of hemoglobin A1c in normal and diabetic mice: potential model of basement membrane thickening. *Proc Natl Acad Sci U S A* 72:3687–3691, 1975
42. Gartner K: Glomerular hyperfiltration during the onset of diabetes mellitus in two strains of diabetic mice (c57bl/6j db/db and c57bl/ksj db/db). *Diabetologia* 15:59–63, 1978
43. Abdel-Wahab N, Weston BS, Roberts T, Mason RM: Connective tissue growth factor and regulation of the mesangial cell cycle: role in cellular hypertrophy. *J Am Soc Nephrol* 13:2437–2445, 2002
44. Suzuma K, Naruse K, Suzuma I, Takahara N, Ueki K, Aiello LP, King GL: Vascular endothelial growth factor induces expression of connective tissue growth factor via KDR, Flt1, and phosphatidylinositol 3-kinase-akt-dependent pathways in retinal vascular cells. *J Biol Chem* 275:40725–40731, 2000
45. Chen S, Lee JS, Iglesias-de la Cruz MC, Wang A, Izquierdo-Lahuerta A, Gandhi NK, Danesh FR, Wolf G, Ziyadeh FN: Angiotensin II stimulates alpha3(IV) collagen production in mouse podocytes via TGF-beta and VEGF signalling: implications for diabetic glomerulopathy. *Nephrol Dial Transplant* 20:1320–1328, 2005
46. Hoffman BB, Sharma K, Zhu Y, Ziyadeh FN: Transcriptional activation of transforming growth factor-beta1 in mesangial cell culture by high glucose concentration. *Kidney Int* 54:1107–1116, 1998
47. Chow F, Ozols E, Nikolic-Paterson DJ, Atkins RC, Tesch GH: Macrophages in mouse type 2 diabetic nephropathy: correlation with diabetic state and progressive renal injury. *Kidney Int* 65:116–128, 2004
48. Banba N, Nakamura T, Matsumura M, Kuroda H, Hattori Y, Kasai K: Possible relationship of monocyte chemoattractant protein-1 with diabetic nephropathy. *Kidney Int* 58:684–690, 2000
49. Clauss M, Gerlach M, Gerlach H, Brett J, Wang F, Familletti PC, Pan YC, Olander JV, Connolly DT, Stern D: Vascular permeability factor: a tumor-derived polypeptide that induces endothelial cell and monocyte procoagulant activity, and promotes monocyte migration. *J Exp Med* 172:1535–1545, 1990
50. Iglesias-de la Cruz MC, Ziyadeh FN, Isono M, Kouahou M, Han DC, Kalluri R, Mundel P, Chen S: Effects of high glucose and TGF-beta1 on the expression of collagen IV and vascular endothelial growth factor in mouse podocytes. *Kidney Int* 62:901–913, 2002
51. Cha DR, Kim NH, Yoon JW, Jo SK, Cho WY, Kim HK, Won NH: Role of vascular endothelial growth factor in diabetic nephropathy. *Kidney Int* 77 (Suppl.):S104–S112, 2000
52. Forbes JM, Bonnet F, Russo LM, Burns WC, Cao Z, Candido R, Kawachi H, Allen TJ, Cooper ME, Jerums G, Osicka TM: Modulation of nephrin in the

diabetic kidney: association with systemic hypertension and increasing albuminuria. *J Hypertens* 20:985–992, 2002
53. Cohen MP, Chen S, Ziyadeh FN, Shea E, Hud EA, Lautenslager GT, Shearman CW: Evidence linking glycated albumin to altered glomerular nephrin and VEGF expression, proteinuria, and diabetic nephropathy. *Kidney Int* 68:1554–1561, 2005
54. Eremina V, Sood M, Haigh J, Nagy A, Lajoie G, Ferrara N, Gerber HP, Kikkawa Y, Miner JH, Quaggin SE: Glomerular-specific alterations of VEGF-A expression lead to distinct congenital and acquired renal diseases. *J Clin Invest* 111:707–716, 2003
55. Satchell SC, Harper SJ, Tooke JE, Kerjaschki D, Saleem MA, Mathieson PW: Human podocytes express angiopoietin 1, a potential regulator of glomerular vascular endothelial growth factor. *J Am Soc Nephrol* 13:544–550, 2002
56. Nosadini R, Velussi M, Brocco E, Abaterusso C, Piarulli F, Morgia G, Satta A, Faedda R, Abhyankar A, Luthman H, Tonolo G: Altered transcapillary escape of albumin and microalbuminuria reflects two different pathogenetic mechanisms. *Diabetes* 54:228–233, 2005
57. Soulie P, Gamelin E, Eder JP, Bonneterre J, Ryan DP, Clark JW, Appleman LJ, Herait P, Marsh S, Jekunen A: A dose finding study of an oral antiangiogenesis inhibitor, NM-3: safety profile and effects on surrogate markers with once-daily dosing. *Proc Am Soc Clin Oncol* 22:194, 2003